J. Membrane Biol. 155, 175–186 (1997)

The Journal of
Membrane
Biology

Presteady-State Currents of the Rabbit Na^+/Glucose Cotransporter (SGLT1)

A. Hazama*, **D.D.F. Loo, E.M. Wright**
Department of Physiology, UCLA School of Medicine, Center for the Health Sciences, Los Angeles, CA 90095-1751

Received: 12 August 1996/Revised: 30 September 1996

Abstract. The rabbit Na^+/glucose cotransporter (SGLT1) exhibits a presteady-state current after step changes in membrane voltage in the absence of sugar. These currents reflect voltage-dependent processes involved in cotransport, and provide insight on the partial reactions of the transport cycle. SGLT1 presteady-state currents were studied as a function of external Na^+, membrane voltage V_m, phlorizin and temperature. Step changes in membrane voltage—from the holding V_h to test values, elicited transient currents that rose rapidly to a peak (at 3–4 msec), before decaying to the steady state, with time constants $\tau \approx$4–20 msec, and were blocked by phlorizin ($K_i \approx$30 μM). The total charge Q was equal for the application of the voltage pulse and the subsequent removal, and was a function of V_m. The Q-V curves obeyed the Boltzmann relation: the maximal charge Q_{max} was 4–120 nC; $V_{0.5}$, the voltage for 50% Q_{max} was −5 to +30 mV; and z, the apparent valence of the moveable charge, was 1. Q_{max} and z were independent of V_h (between 0 and −100 mV) and temperature (20–30°C), while increasing temperature shifted $V_{0.5}$ towards more negative values. Decreasing $[Na^+]_o$ decreased Q_{max}, and shifted $V_{0.5}$ to more negative voltages 9by −100 mV per 10-fold decrease in $[Na^+]_o$). The time constant τ was voltage dependent: the τ-V relations were bell-shaped, with maximal τ_{max} 8–20 msec. Decreasing $[Na^+]_o$ decreased τ_{max}, and shifted the τ-V curves towards more negative voltages. Increasing temperature also shifted the τ-V curves, but did not affect τ_{max}. The maximum temperature coefficient Q_{10} for τ was 3–4, and corresponds to an activation energy of 25 kcal/mole. Simulations of a 6-state ordered kinetic model for rabbit Na^+/glucose cotransport indicate that charge-movements are due to Na^+-binding/dissociation and a conformational change of the empty transporter. The model predicts that (i) transient currents rise to a peak before decay to steady-state; (ii) the τ-V relations are bell-shaped, and shift towards more negative voltages as $[Na^+]_o$ is reduced; (iii) τ_{max} is decreased with decreasing $[Na^+]_o$; and (iv) the Q-V relations are shifted towards negative voltages as $[Na^+]_o$ is reduced. In general, the kinetic properties of the presteady-state currents are qualitatively predicted by the model.

Key words: Na^+/glucose cotransport — Kinetic model — Presteady-state kinetics — Charge movement

Introduction

Glucose is actively transported across the brush border membrane of the intestine and late proximal tubule by the Na^+/glucose cotransporter (SGLT1). SGLT1 is representative of a wide class of integral membrane proteins which uses the electrochemical potential gradient for ions (Na^+ and H^+) to accumulate organic substrates (sugars, amino acids, neurotransmitters and osmolytes) in cells. Electrophysiological studies of the steady-state kinetic properties of the cloned rabbit, rat and human SGLT1 expressed in *Xenopus* oocytes indicate that cotransporter activity is dependent on membrane voltage (Umbach, Coady & Wright, 1990; Birnir, Loo & Wright, 1991; Parent et al., 1992*a;* Hirayama, Loo & Wright, 1995; Panayotova-Heiermann, Loo & Wright, 1995). SGLT1 also exhibits a presteady-state current after step changes in membrane voltage in the absence of sugar (Birnir et al., 1991; Parent et al., 1992*a;* Loo et al., 1993; Lostao et al., 1994; Panayotova-Heiermann et al., 1994, 1995). Presteady-state currents reflect voltage-dependent processes involved in cotransport such as ion binding and conformational transitions of the cotransporter,

* *Present address:* National Institute for Physiological Sciences, Department of Cell Physiology, Okazaki, 444, Japan

Correspondence to: D.D.F. Loo

and provide insights on the partial reactions of the transport reaction cycle.

A six-state ordered kinetic model has been proposed for Na^+-dependent sugar transport (Parent et al., 1992*b*; Loo et al., 1993). According to this model, membrane voltage affects Na^+ binding to the transporter and conformational transitions of the unloaded transporter between external and internal membrane surfaces. Thus presteady-state currents observed after step changes in membrane voltage are due to charge movements caused by binding/dissociation of external Na^+ and the conformational change involved in the reorientation of the ligand binding sites of the cotransporter in the membrane. We have previously described the presteady-state currents of the human Na^+/glucose cotransporter (Loo et al., 1993). However, the median voltage ($V_{0.5}$) of the presteady-state charge movement was at −40 mV (at 100 mM external sodium concentration), making the detailed analysis of the dependence of the presteady state kinetics on membrane voltage and sodium concentration problematic. This problem is solved by the use of the rabbit SGLT1, which has a $V_{0.5}$ between −5 to +30 mV. Our aim in this study was to extend our previous study and to test the kinetic model by measuring the rabbit SGLT1 presteady-state kinetics as a function of voltage, sodium concentration, temperature and phlorizin concentration.

Materials and Methods

The rabbit intestinal Na^+/glucose transporter (rSGLT1, Hediger et al., 1987) was expressed in *Xenopus* oocytes, and experiments were performed on oocytes 5–14 days after injection of cRNA. Oocytes were bathed in a buffer containing (mM): 100 NaCl, 2 KCl, 1 $CaCl_2$, 1 $MgCl_2$, and 10 Hepes (pH 7.4). The composition of the bathing solution was varied by replacing NaCl (100–0 mM) with choline chloride and/or adding phlorizin.

Electrophysiological experiments were performed using the two electrode voltage clamp (Loo et al., 1993). The voltage clamp amplifier maintained the interior of the oocyte at earth potential and had a settling time of 0.5–0.8 msec for a 100-mV step voltage pulse (Loo et al., 1993). All potentials are expressed relative to the bath solution. Presteady-state currents were studied using a pulse protocol. Membrane voltage was stepped from the holding (V_h) to a series of test values V_t varying from +50 to −150 mV in 20 mV decrements. The current at each test voltage was averaged from 15 sweeps, low-pass filtered at 5 kHz by a 8-pole Bessel filter and digitized at 100 μsec per point.

Oocyte membrane capacitance was determined by applying 10–20 mV hyperpolarizing voltage pulses from the holding potential (−100 mV). The charge Q (at each test voltage) was obtained by integration of the capacitive transient. In control H_2O-injected and noninjected oocytes, capacitive transients showed a single time constant (≈0.5 msec), and Q was a linear function of the voltage step (V_t–V_h). The slope of the Q *vs.* (V_t–V_h) relation was the membrane capacitance C_m.

In SGLT1 cRNA-injected oocytes, besides the capacitive transient (time constant τ ~ 0.8 msec) the total transient current relaxation contained two additional components: a rapid rise to a peak with τ_{fast} ~ 100 μsec, and a slow decay to the steady-state with τ_{slow} ~ 10 msec (Loo et al., 1993; *see also* Fig. 1*B*). The presteady-state current of SGLT1 was isolated from the total current either by point to point subtraction of the total currents in the presence and absence of phlorizin, a specific inhibitor of SGLT1, or the total current $I(t)$ was fitted by $I(t) = I_1 e^{-t/\tau 1} + I_2 e^{-t/\tau 2} + I_{ss}$, where I_1 is the capacitance current with time constant τ_1, t is time, I_2 is the SGLT1 transient current with time constant τ_2, and I_{ss} is the steady-state current. In this approximation to the total current, τ_2 corresponds to the slow time constant τ_{slow} as the fast time constant τ_{fast} was beyond the resolution of the two-electrode voltage clamp. SGLT1 presteady-state current was obtained from $I(t)$ by substraction of the capacitive and steady-state components $I(t)$-$I_1 e^{-t/\tau 1} - I_{ss}$). Presteady-state currents and charge movements were similar for the two methods (Loo et al., 1993). Nonlinear fits of the data were performed using SigmaPlot (Jandel, San Rafael, CA). In general, each of the results described was for experiments carried out in one oocyte, but all were performed at least three times on oocytes from different donor frogs.

Mathematical Modeling

Model simulations of the 6-state kinetic model were performed by numerical integration, using the Runge-Kutta method (Press et al., 1988), of the differential equations describing the time evolution of the transporter states ([C]′, [C]″, [CNa_2]′, *see* Fig. 6) after step changes in membrane voltage (Eqs. A44–A50, Parent et al., 1992*b*; Loo et al., 1993). The charge Q was obtained by integration of the current equation (Eq. A50, Parent et al., 1992*b*) in response to a step change in membrane voltage. The time constants for the presteady-state relaxation currents (Fig. 7*B* and *F*) were obtained directly from solving for the eigenvalues of the 3-state model ([CNa_2]′ ⇄ [C]′ ⇄ [C]″) indicated by the shaded region in Fig. 6 (Loo et al., 1993).

Results

Figure 1*A* shows the total current records as the membrane voltage was stepped from the holding (−100 mV) to test values (+50, −30, −70, −110 and −150 mV) in a rSGLT1 cRNA-injected oocyte in 100 mM NaCl buffer in the absence of sugar at 25°C. The current relaxation consisted of an initial capacitive spike (time constant τ ~0.8 msec) followed by a slower decay (τ ~10 msec) to the steady state. This slow component is the presteady-state current of rSGLT1. It was not observed in H_2O-injected oocytes, and was blocked by phlorizin (*see* Fig. 5 below) and sugar (α-methyl-D-glucopyranoside, Birnir et al., 1991; Parent et al., 1992*a;* Loo et al., 1993; Lostao et al., 1994). Figure 1*B* shows the rSGLT1 presteady-state currents, isolated from the total current using the fitted method (*see* Materials and Methods). At large depolarizing voltages (e.g., at +30 and +50 mV), the current initially rose to a peak (at 3–4 msec) before decaying to the steady state. With hyperpolarizing voltages, there was virtually no presteady-state current. Thus the current relaxation consisted of three components: an initial fast component (τ ≈0.8 msec) due to membrane capacitance and was voltage independent (*data not shown*); a rise to the peak; and then a slower decay to the steady-state. For the ON-response, the time constant of the slow component was voltage dependent and is shown in Fig.

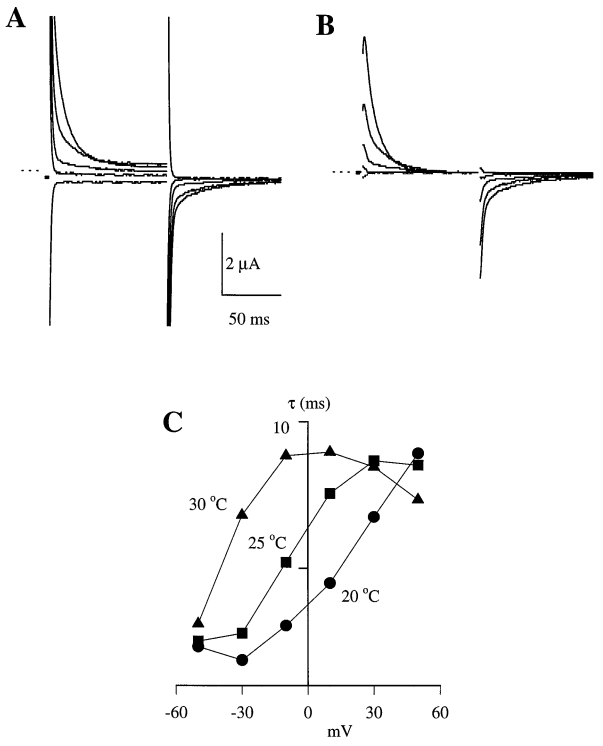

Fig. 1. Presteady-state currents in an oocyte injected with rabbit SGLT1 cRNA. (*A*) Total currents in an oocyte as the membrane potential was held at $V_h = -100$ mV and stepped to test potentials V_t (+50, +10, −30, −110 and −150 mV). Bath solution contained 100 mM NaCl without sugar and was maintained at 25°C. (*B*) Transporter-mediated charge movement. These were obtained from the total current in Fig. 1*A* by subtraction of the capacitive and steady-state currents using the fitted method, and are displayed 1.6 msec after the voltage step. At this time, the ratio of the transient to capacitive current was greater than 4 at $V_t = +50$ mV. The dashed lines of (*A*) and (*B*) indicate the zero current level. (*C*) Voltage dependence of the relaxation time constant τ. τ was obtained by fitting the total current $I_{tot}(t)$ during the onset of the voltage pulse to the equation: $I_{tot}(t) = I_1 e^{-t/\tau 1} + I_2 e^{-t/\tau 2} + I_{ss}$. I_1 and τ_1 are the initial currents and time constants of the membrane capacitive current; I_2 and τ_2 are the initial currents and time constants of presteady-state current due to rSGLT1 (*see* Materials and Methods). I_{ss} is the steady-state current. τ_1 was ~0.5 msec and was independent of the test voltage V_t. τ_2 is plotted against V_t at 20°C (circles), 25°C (squares) and 30°C (triangles).

1*C* (■), corresponding to the current records of Fig. 1*A* (at 25°C). τ increased from ≈2 msec at −50 mV to a maximum τ_{max} of 9 msec at +30 mV. There was a wide variation in τ_{max} among oocytes, and was in the range 8–20 msec. In the OFF-response, τ was independent of voltage, e.g., in Fig. 1*B*, τ_{OFF} was 21 ± 2 msec ($n = 3$).

Both membrane capacitance and rSGLT1 presteady-state transients contribute to the total charge transfer, obtained as the integral of the total current relaxation (Fig. 2*A*, ●). The charge *Q* due to rSGLT1 can be obtained by integration of the presteady-state currents (Fig. 1*B*). Alternatively, since there was no presteady-state currents for hyperpolarizing voltages (*see* Fig. 1), *Q* can be isolated from the total charge by subtracting the linear component of the membrane capacitance (Fig. 2*A*, broken line). Phlorizin abolished the presteady-state current (Fig. 2*B*), thus *Q* can also be obtained as the difference in total charge in the presence and absence of phlorizin. To illustrate the equivalence of the two methods, Fig. 2*B* shows the total charge in the presence of phlorizin (0.5 mM phlorizin). The *Q-V* relation is linear with slope 315 nF. This is close to the value of 318 nF which is the linear component of the membrane capacitance (Fig. 2*A*). Thus the charge-voltage (*Q-V*) relation of SGLT1, obtained as the difference in *Q* in presence and absence of phlorizin, is the same as the *Q-V* curve obtained by subtracting the linear component of membrane capacitance from the total charge.

Figure 2C (■) shows the charge-voltage (*Q-V*) relation for the current records of Fig. 1*A* (at 25°C). The curve is sigmoidal, and the data were fitted (solid smooth curve) to the Boltzmann relation: $(Q\text{-}Q_{hyp})/Q_{max} = 1/[1 + \exp(z(V - V_{0.5})F/RT]$. $Q_{max} = Q_{dep} - Q_{hyp}$. Q_{dep} and Q_{hyp} being *Q* at depolarizing and hyperpolarizing limits. $V_{0.5}$ is the voltage for 50% charge transfer and *z*, the apparent valence of the movable charge. Q_{max} was 60 nC, $z = 1.1$ and $V_{0.5}$ was +10 mV. Among oocytes, there was a wide variation in $V_{0.5}$ which ranged from −5 to +30 mV (at 100 mM $[Na]_o$).

The dependence of *Q* on the holding potential V_h (at 30°C and from a different oocyte) is shown in Fig. 2*D*. *Q* was equal for the ON- and OFF-responses (filled and open symbols of Fig. 2*D*) for all test voltages. As V_h was made more negative, the hyperpolarizing and depolarizing limits (Q_{hyp} and Q_{dep}) shifted in parallel towards more negative values, but there was no change in Q_{max} (42 ± 1 nC, $n = 3$). Likewise there were no changes in $V_{0.5}$ and *z*, and were −36 ± 1 mV ($n = 3$) and 1.07 ± 0.03 ($n = 3$), respectively.

Dependence on $[Na]_o$

The dependence of presteady-state currents on external Na^+ ($[Na^+]_o$) is illustrated in Fig. 3. The current records at 100 and 20 mM $[Na]_o$ (Fig. 3*A* and *B*) are shown at V_t +50, +30, −110 and −130 mV. The peak current in the depolarizing direction (e.g., at +50 mV) decreased as $[Na^+]_o$ was reduced from 100 to 20 mM but increased in the hyperpolarizing direction. There was no difference in the time to peak current between 100 mM and 20 mM $[Na^+]_o$ (4.2 *vs.* 4.3 msec). The family of *Q-V* curves as $[Na]_o$ was reduced from 100 to 10 mM is shown in Fig. 3*C*. For comparison, they have been normalized to the extrapolated depolarizing limit (Q_{dep}, 60 nC) at 100 mM $[Na]_o$, and have been shifted to align at Q_{dep}. The maximal charge Q_{max} decreased with a reduction in external Na^+ (Fig. 3*E* and Table 1) and the voltage for 50% maximal charge $V_{0.5}$ shifted towards more negative values (Fig. 3*D*). For instance, in the experiment represented by the filled circles (●) which was performed at 25°C, a

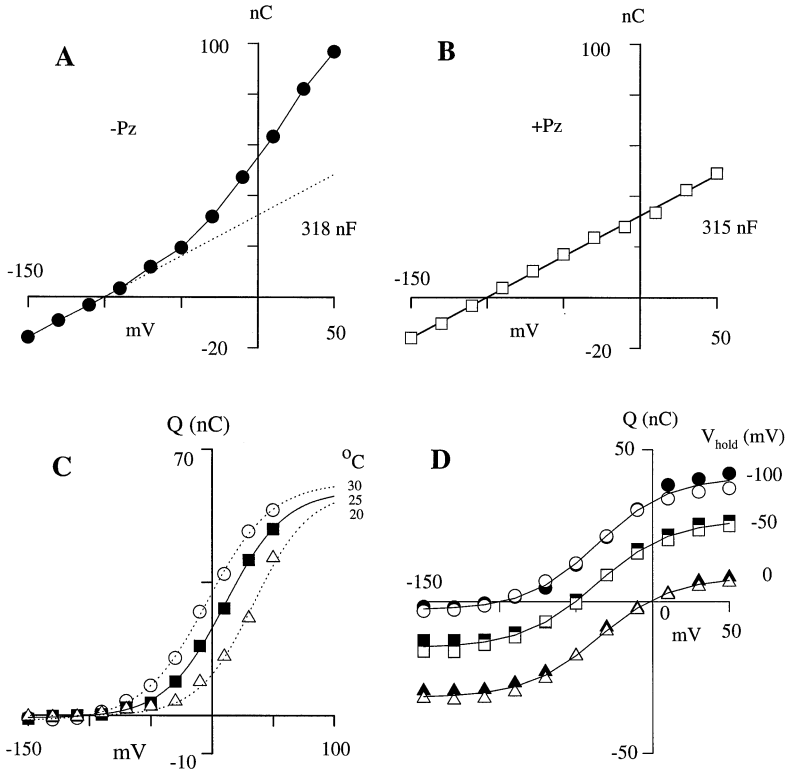

Fig. 2. Estimation of charge transfer *Q*. (*A*) Total charge *Q* vs. voltage (*Q-V*) relationship. *Q* (●) was obtained by integration of the total transient current in response to a voltage jump. The broken line was obtained by linearization of the *Q-V* relation when the test voltage V_t was more negative than −100 mV. The slope was 318 nF. Bath solution was 100 mM NaCl in absence of sugar, at 25°C. (*B*) Total charge *Q* obtained after addition of 0.5 mM phlorizin to the bathing solution. This experiment was performed on the same oocyte as Fig. 2*A*. The line was drawn by linear regression with slope 315 nF. (*C*) *Q-V* relation of rSGLT1 was obtained by subtraction of the total charge in presence and absence of 0.5 mM phlorizin (□, Fig. 2*B*). The curve was the same when obtained by subtraction of the linear component from the total charge *Q*. *Q* was also the same when obtained by integration of the current transients of SGLT1 using the fitted method. At each V_h, the data were fitted (smooth curves) to the Boltzmann relation: $(Q-Q_{hyp})/Q_{max} = 1/[1 + \exp(z(V - V_{0.5})F/RT]$. $Q_{max} = Q_{dep} - Q_{hyp}$. Q_{dep} and Q_{hyp} being *Q* at depolarizing and hyperpolarizing limits, and varied with V_h. *F*, Faraday's constant; *R*, the gas constant; *T*, absolute temperature; $V_{0.5}$, the potential for 50% charge transfer; and *z*, the apparent valence of the moveable charge. At 20°C, Q_{max} = 59 nC, $V_{0.5}$ = 34 mV, and z = 1.1; at 25°C, Q_{max} = 60 nC, $V_{0.5}$ = 10 mV, and z = 1.1; and at 30°*C*, Q_{max} = 64 nC, $V_{0.5}$ = −4 mV, and z = 1.0. The oocyte membrane capacitance was 315 nF. (*D*) Dependence of *Q* on holding potential. The ON- and OFF- charges Q_{on} and Q_{off} are represented by the filled and open symbols respectively. At each V_h, the curves were drawn by fitting the Boltzmann relation to the mean of Q_{on} and Q_{off}. At V_h = −100 mV: Q_{max} = 44 nC, z = 1.1 and $V_{0.5}$ = −35 mV. At V_h = −50 mV: Q_{max} = 42 nC, z = 1.0, $V_{0.5}$ = −37 mV. At V_h = 0 mV: Q_{max} = 40 nC, z = 1.1, $V_{0.5}$ = −35 mV. Temperature was 30°C. The experiment was performed on a different oocyte from that of Fig. 2*C*.

10-fold reduction in $[Na]_o$ from 100 to 10 mM shifted $V_{0.5}$ by 98 mV (from +10 to −88 mV), and decreased Q_{max} 46% (from 50 nC to 32 nC). *z*, the apparent valence of the moveable charge was not affected and was 1.1 ± 0.1 (n = 4).

Figure 4*B* shows the τ-*V* relations as $[Na]_o$ was varied between 10 to 100 mM at 25°C. The peak of the τ-*V* curves, i.e., the maximal time constant τ_{max}, decreased (Table 1), and the τ-*V* curves shifted towards more negative potentials as $[Na]_o$ was lowered. There is a shift of 60 mV in V_{max} (voltage at τ_{max}) from +30 mV at 100 $[Na]_o$ to −30 mV at 20 mM $[Na]_o$ (Table 1). Consequently, the effect of lowering $[Na]_o$ on τ depended on voltage and temperature. At +10 mV τ decreased as $[Na]_o$ was reduced, whereas at −50 mV, τ increased.

Dependence on Temperature

Temperature affected charge movement by shifting the median voltage $V_{0.5}$ of the charge-voltage relations. Figure 2*C* shows the *Q-V* curves in one experiment as temperature was increased from 20 to 30°C with $[Na]_o$ maintained at 100 mM. There was a shift of $V_{0.5}$ from +34 mV at 20°C to −4 mV at 30°C whereas Q_{max} and *z* were unaffected (Table 1).

Temperature influenced the rate of relaxation of the presteady-state currents. Figure 1*C* shows a shift of the τ-*V* curves towards more negative voltages as temperature increased from 20 to 30°C. This shift is similar (≈40 mV) to the shift of the *Q-V* curves. Temperature had differential effects on relaxation kinetics: for potentials more negative than +30 mV, increasing temperature increased τ, and at +50 mV, τ decreased with increasing temperature.

Figure 4*D* shows the temperature coefficient (Q_{10}) for the time constant τ as a function of membrane voltage. Q_{10} was maximal at 100 mM $[Na]_o$. Maximal Q_{10} was *ca.* 4 at 100 mM $[Na]_o$ and −30 mV, and at each $[Na]_o$ Q_{10} decreased to 1 as membrane voltage was made more positive. At each voltage (between −30 and +30 mV), lowering of $[Na]_o$ decreased Q_{10}. At the lowest $[Na]_o$ studied ($[Na]_o$ = 10 mM), Q_{10} was 1 and relatively independent of voltage.

Blockade by Phlorizin

Phlorizin is a high affinity blocker ($K_i \approx 10$ μM) of the steady-state sugar-induced currents generated by

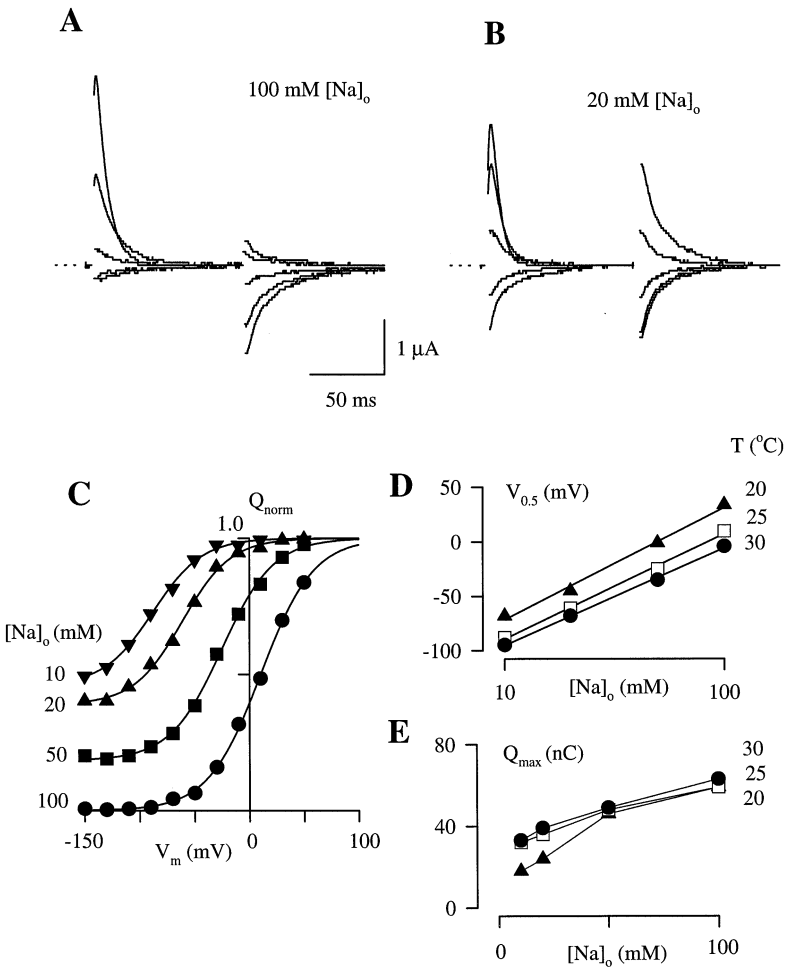

Fig. 3. Dependence of presteady-state currents on $[Na^+]_o$. (*A* and (*B*) Presteady-state current records, obtained using the fitted method, are depicted at test potentials V_t (+50, +30, −110, and −130 mV) from the holding potential $V_h = -50$ mV at 100 mM $[Na^+]_o$ (*A*) and 20 mM $[Na^+]_o$ (*B*). Temperature was 25°C. External Na^+ was replaced iso-osmotically with choline. (*C*) Normalized *Q-V* relations when bath contained 100 (circles), 50 (squares), 20 (triangles) and 10 mM $[Na^+]_o$ (inverted triangles). The curves are drawn according to the Boltzmann relation. For comparison, they have been normalized to the maximal charge (59 nC) at the depolarizing limit at 100 mM $[Na^+]_o$ and have been shifted so that they aligned at the depolarizing limit. (*D*) Dependence of $V_{0.5}$ on $[Na^+]_o$. (*E*) Dependence of Q_{max} on $[Na^+]_o$.

Table 1. Dependence of kinetics on $[Na]_o$ and temperature

T (°C)	20°				25°				30°			
$[Na]_o$(mM)	100	50	20	10	100	50	20	10	100	50	20	10
Q_{max} (nC)	59	46	24	18	59	48	36	32	63	49	39	33
$V_{0.5}$ (mV)	34	−1	−45	−68	10	−25	−61	−88	−4	−35	−68	−95
−z	1.1	1.1	1.2	1.2	1.1	1.1	1.1	1.1	1.0	1.0	1.1	1.2
τ_{max} (msec)		7.6	6.1	4.4	8.7	7.5	6.2	9.0	7.9			
$V_{\tau max}$		50	−10	−30	30	10	−30		10	−30		

τ_{max} is the maximal τ, which is the slow time constant. $V_{\tau max}$ is the membrane voltage at τ_{max}. The columns with no entries mean that the parameters were beyond the data range.

rSGLT1 (Umbach et al., 1990; Birnir et al., 1991; Parent et al., 1992*a*). Phlorizin also blocks the presteady-state currents of rSGLT1. This is illustrated in Fig. 5*A* and *B* which shows the presteady-state currents in absence of phlorizin (*A*) and with 50 μM phlorizin (*B*) in the bath solution. Membrane potential was held at −100 mV at 30°C. Figure 5*C* shows the *Q-V* relationship as external phlorizin varied from 0 to 100 μM. Q was reduced. Of the Boltzmann parameters, Q_{max} was reduced with increasing $[phlorizin]_o$, but *z* and $V_{0.5}$ were unaffected, 0.94 ± 0.08 ($n = 5$) and −4.0 ± 0.8 mV ($n = 5$) respectively. The reduction of Q_{max} with $[phlorizin]_o$ followed a hyperbolic relationship with a K_i of 28 μM and was relatively independent of membrane voltage. Thus inhibition of charge movement by phlorizin was independent of voltage (between −30 to +50 mV).

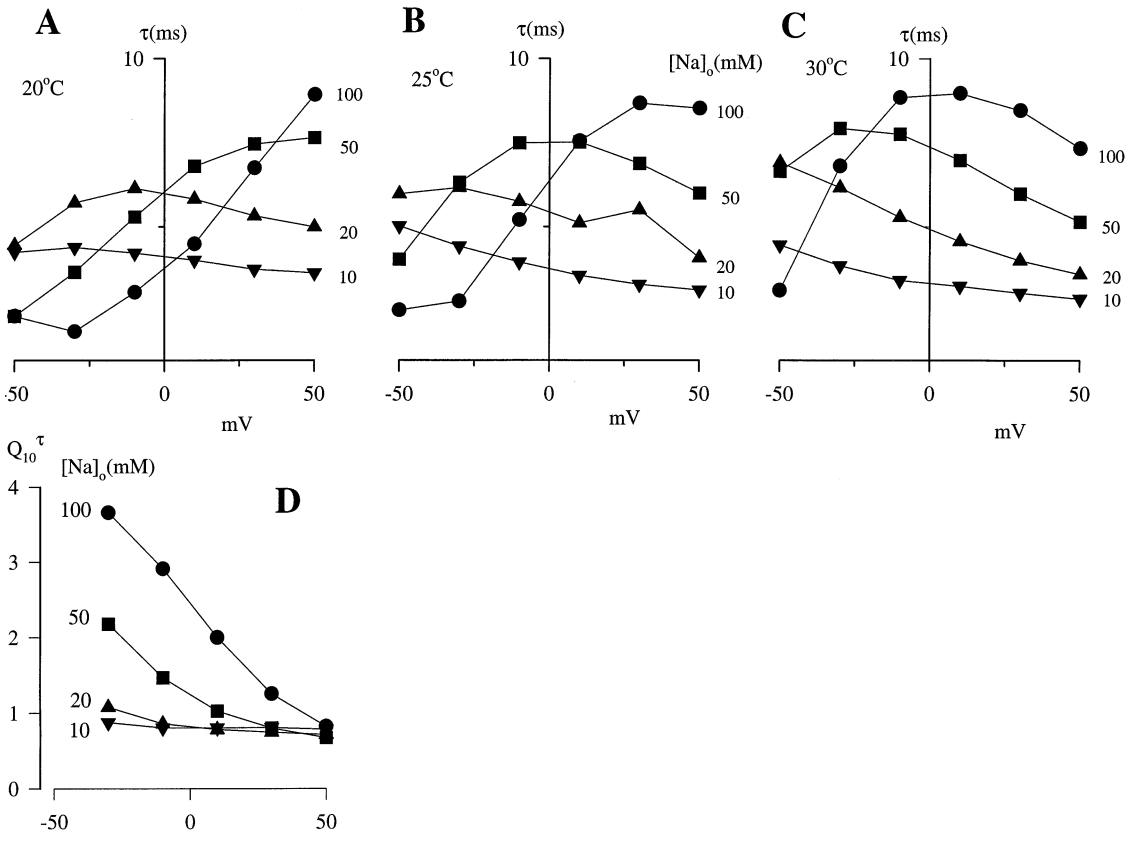

Fig. 4. Dependence of τ on temperature. Dependence of τ on $[Na]_o$ as bath temperature was maintained at 20 (*A*), 25 (*B*) and 30°C (*C*). V_h was −100 mV. (*D*) Dependence of the temperature coefficient Q_{10} for τ on membrane voltage and $[Na]_o$. Q_{10} was defined by the relation: $Q_{10} = \tau(30°C)/\tau(20°C)$. Data were obtained on the same oocyte as Fig. 4*A* with $V_h = -100$ mV. These results are summarized on Table 1.

Discussion

Presteady-state Currents are Due to SGLT1 Charge Movement

The following observations provide compelling evidence that the presteady-state currents are due to the SGLT1 intramembrane charge movement: (i) presteady-state currents are observed in SGLT1-cRNA injected oocytes, but not in control H_2O-injected or non-injected oocytes (Parent et al., 1992*a;* Loo et al., 1993; Panayotova-Heiermann et al., 1995); (ii) presteady-state currents are eliminated by phlorizin (Fig. 5), a specific competitive blocker of Na^+/glucose cotransport; (iii) presteady-state currents are blocked by substrates such as glucose (Loo et al., 1993; Lostao et al., 1994); (iv) charge movements, obtained as the integral of the presteady-state currents, as a function of membrane voltage, fitted the Boltzmann relation with a Q_{max} in the range (4–120 nC), a $V_{0.5}$ of +10 mV (range −5 to +30 mV), and z of 1.1 (Fig. 2); (v) the ON- charges are equal and opposite to the OFF-charges ((Fig. 2*D*); (vi) the maximal charge Q_{max}, the median voltage $V_{0.5}$ and the apparent valence z are independent of the holding potential between −100 and 0 mV (Fig. 2*D*); (vii) Q_{max} is independent of temperature between 20 and 30°C (Fig. 2*C*), but the time constant τ for presteady-state current relaxations are temperature sensitive (Fig. 4); and (viii) Q_{max} is proportional, over a 100-fold range, to the level of SGLT1 expression, as measured by the maximum sugar-induced current I_{max} (Loo et al., 1993; Hirsch, Loo & Wright, 1996). The ratio I_{max}/Q_{max} is the turnover number of the transporter (25/sec for rabbit SGLT1) (Loo et al., 1993; Panayotova-Heiermann et al., 1994); and (ix) Q_{max} is proportional to the increase in the number of 7.5 nm diameter intramembrane particles in the protoplasmic-free of the oocyte plasma membrane (Zampighi et al., 1995).

Presteady-state currents are a general property of cotransporters, and have been measured in several gene families (Table 2). These include the transporters for sugars (glucose and myoinositol), neurotransmitters and amino acids (norepinephrine, glutamate, GABA, taurine and betaine), peptides (dipeptide) and anions (iodide), as well as a plant proton-dependent hexose transporter (Boorer, Loo & Wright, 1994). In all these cotransporters, presteady-state currents share a number of common properties: (i) they are abolished by the transported sub-

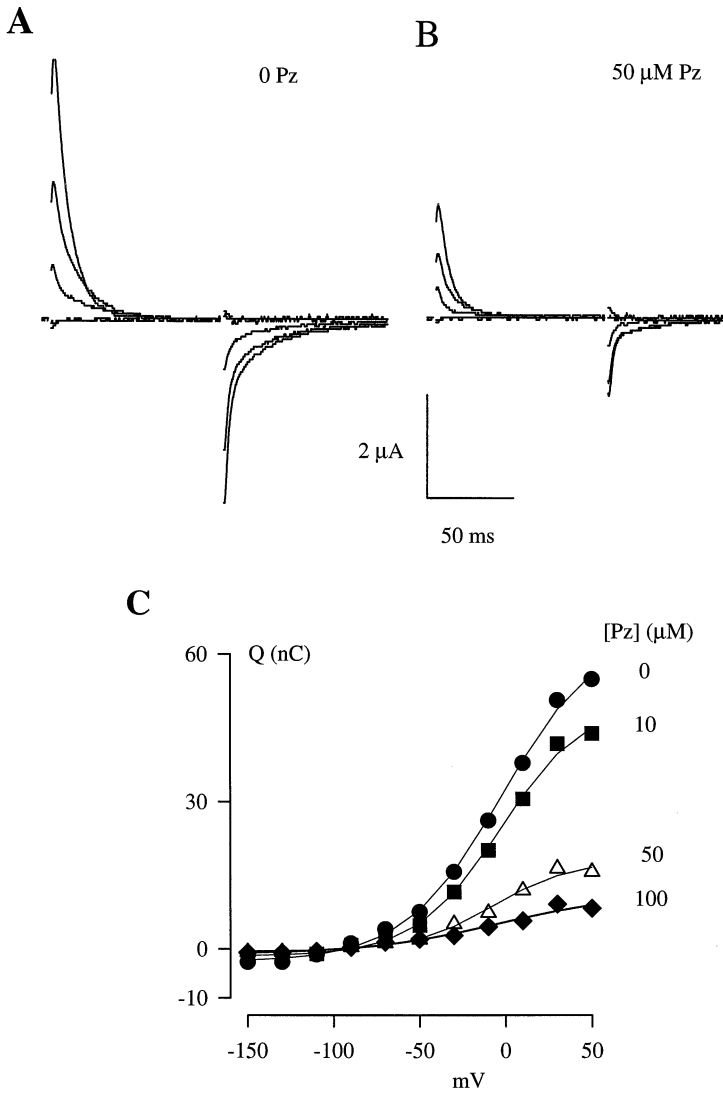

Fig. 5. Blockade of presteady-state currents by phlorizin. (*A*) Presteady-state currents in absence of phlorizin. (*B*) Presteady-state currents with 50 μM phlorizin added to the bath solution. (*C*) *Q-V* relations at different $[phlorizin]_o$. The curves were drawn according to the Boltzmann relation. *z*, and $V_{0.5}$ were independent of membrane voltage and $[phlorizin]_o$. Experiment was performed at 100 mM NaCl at 30°C.;

strates and/or blockers; (ii) the maximal charge movement Q_{max} apparently decreased by decreasing $[Na^+]_o$ (or $[H^+]_o$); (iii) $V_{0.5}$, the voltage for 50% Q_{max}, shifted towards more negative membrane potentials as $[Na^+]_o$ (or $[H^+]_o$) is decreased; and (iv) in freeze-fracture studies of the transporters expressed in oocytes, Q_{max} was proportional to the number of intramembrane particles (Zampighi et al., 1995). It is interesting to note that the apparent valence of the moveable charge *z* is close to 1 for all the transporters that have been studied (*see* Table 1 of Mackenzie et al., 1995), with the exception of the Na^+/glucose transporter where $z = 0.4$ (Wadiche et al., 1995) and the Na^+/norepinephrine transporter where the *Q-V* relations have not been shown to obey the Boltzmann relation (Galli et al., 1995). The magnitude of the shift in $V_{0.5}$ for a tenfold reduction in $[Na^+]_o$ (or $[H^+]_o$) was similar (*ca.* 100 mV) between the rabbit Na^+/glucose (*present study*), the rat Na^+/Cl^-/GABA (Mager et al., 1993), the low affinity Na^+/glucose (SGLT2, Mackenzie et al., 1995), the H^+/peptide (Mackenzie et al., 1995), and the Na^+/glutamate (Wadiche et al., 1995) transporters. The slow time constant τ_{slow} for presteady-state current relaxation was in the range 4 to 100 msec. In view of these similarities, the origin of presteady-state currents may be similar between the different cotransporters.

Model for SGLT1 Charge Movement

It has been shown that the current generated by the Na^+/glucose cotransporter and the apparent affinities for Na^+ and glucose are dependent on membrane voltage (Umbach et al., 1989; Birnir et al., 1991; Parent et al., 1992*a*), thus at least one of the partial reactions in the transport cycle is voltage-dependent. We have proposed a 6-state ordered kinetic model for Na^+/glucose cotransport (Parent et al., 1992*b*). The model assumes that the transporter (C) is negatively charged (valence-2), and that 2

Table 2. Generality of presteady-state currents

Cotransporter family	Substrate	$V_{0.5}$ (mV)	$\Delta V_{0.5}$(mV)	$V_{\tau max}$ (mV)	τ_{max} (msec)	Reference
Neutral substrates						
SGLT1	Na^+/glucose	+10	−100	+30	9	This study[a]
SGLT2	Na^+/glucose	>+50	≈−100		>15	Mackenzie et al., 1996
SMIT	Na^+/*myo*-inositol	−49		≈−10	14	Hager et al., 1995
Monoamine and amino acids						
NET1	Na^+/norepinephrine					Galli et al., 1995
EAAT2	Na^+/glutamate	+3	≈−130	≈−20	4	Wadiche et al., 1995
GAT1	Na^+/Cl^-/GABA	−27	−100		70–150	Mager et al., 1993[b]
TAUT1	Na^+/Cl^-/taurine	≈+50			40	[c]
BET1	Na^+/Cl^-/betaine	≈−50				[d]
Anions						
NIS	Na^+/iodide	−10		−50	18	[e]
Peptides						
PEPT1	H^+/dipeptide	+30	−80	+43	11	Mackenzie et al., 1995
Plant transporters						
STP1	H^+/hexose	−28		+50	12	Boorer et al., 1994

$V_{0.5}$, $V_{\tau max}$ and τ_{max} were determined at 100 mM NaCl for Na^+-driven transporters and at 3.2 or 10 μM H^+ (pH 5.5, 5.0) for H^+-driven transporters. $\Delta V_{0.5}$ is the shift in $V_{0.5}$ with a 10-fold reduction in extracellular activator concentration.

[a] for rabbit SGLT1. The corresponding values for the human SGLT1 were −39 mV, −31 mV, −50 mV, and 11 msec (Loo et al., 1993) and for the rate were −43, −, −50, and 15 msec (Panayotova-Heiermann et al., 1995).

[b] for rat GAT1. Values for human brain GAT1 were 0–30 mV, −100 mV, −30 mV, and 140–190 msec (D.D.F. Loo, K. Boorer, and E.M. WRight, *unpublished observations).*

[c] D.D.F. Loo, K. Boorer, and E.M. Wright, *unpublished observations.*

[d] A. Hazama, D.D.F. Loo, and E.M. Wright, *unpublished observations.*

[e] S. Eskandari, N. Carrasco, D.D.F. Loo, G. Dai, O. Levy and E.M. Wright, *in preparation.*

Na^+ ions bind to the transporter before sugar binds. The fully-loaded transporter (CNa_2S) undergoes a conformational change, releasing the sugar and the Na^+ ions. The ligand binding sites undergo a conformational change from the internal to the external membrane surface. The 2 voltage-dependent steps in the transport cycle (Fig. 6) are the binding of the Na^+ ions to the outward facing SGLT1 protein in the membrane, and the conformational changes of the SGLT1 protein between the external and internal faces of the membrane. Voltage dependence is given by the exponential dependence of the rate constants for Na^+ association and dissociation (k_{12} and k_{21}) and for the conformational change of the ligand binding sites (k_{16} and k_{61}) on membrane voltage via $e^{\pm 0.3FVm/RT}$ and $e^{\pm 0.7FVm/RT}$, where 0.3 and 0.7 are the fractions of the membrane electric field sensed by Na^+ binding (or dissociation) and the conformational changes of the unloaded protein (Fig. 6). For simplicity, we describe the binding of 2 Na^+ ions as a single reaction step (*see* Parent et al., 1992*b*), that is, either the two Na^+ binding sites are identical or that the binding of the first Na^+ ion is much faster than the other.

Model simulations (as described in Materials and Methods) show that at $V_m = -50$ mV, cell interior negative with respect to the external solution, $[Na]_o = 100$ mM and $[Na]_i = 10$ mM, about 75% of SGLT1 is in state $[CNa_2]'$, 15% is in state $[C]'$ and 7% is in state $[C]''$. The model predicts that the transient currents observed with depolarizing voltage steps are due to dissociation of Na^+ from the transporter ($[CNa_2]' \rightleftarrows [C]'$), and reorientation of the protein in the membrane ($[C]' \rightleftarrows [C]''$. 30% of the charge movement is due to Na^+ dissociation and 70% is due to the conformational change. On restoring the membrane voltage to the holding value at the end of the voltage pulse, the OFF transient currents are simply due to the reversal of the process. The addition of saturating amounts of glucose or the inhibitor phlorizin to the external solution dramatically alters the distribution of the cotransporter between the six states—at 100 mM $[Na]_o$ and −50 mV the addition of 1 mM sugar results in the steady-state distribution with 40% in state $[CNa_2]''$, 20% in state $[CNa_2S]'$ and 21% in state $[C]''$. Thus the charge movement in response to stepping the voltage from −50 to +50 is dramatically diminished.

Estimates of the rate constants have been obtained by numerical simulations of the presteady-state and steady-state kinetics of human, rabbit and rat Na^+/glucose cotransporters (Parent et al., 1992*b;* Loo et al., 1993; Panayotova-Heiermann et al., 1994). The goal of the present study was to further test the validity of the model by measuring rabbit SGLT1 charge movements as a function of $[Na]_o$ and $[phlorizin]_o$ and temperature. The experimental results were compared and contrasted with the predictions of our model.

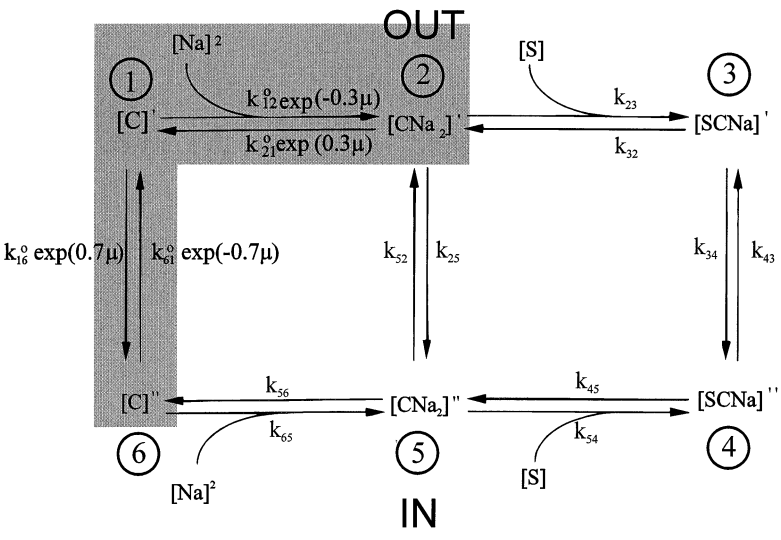

Fig. 6. Transport model for SGLT1. A six-state ordered kinetic model where two Na^+ ions bind to the transporter (valence −2) before the binding of sugar. $\mu = FV/R$; V is membrane voltage; F, R, and T have their usual physicochemical meanings. The empty transporter [C], the Na^+-loaded transporter [CNa_2], and the sugar-loaded transporter [CNa_2S] can cross the membrane. Membrane voltage effects Na^+ binding with the transporter and translocation of the empty transporter across the membrane. The following observations support the hypothesis that the partial reactions in the shaded region are involved in the generation of the presteady-state currents: (i) presteady-state currents are observed in the absence of sugar; (ii) the rate constants for the sugar-uncoupled Na^+ current ($[CNa_2]' \rightleftarrows [CNa_2]''$) are low and independent of voltage ($k_{25} = .01$ sec^{-1} and $k_{52} = 0.56$ sec^{-1}, Panayotova-Heiermann et al., 1994); and (iii) internal [Na] is low (~5 mM) and the reaction $[C]'' \rightleftarrows [CNa_2]'$ is insensitive to voltage (Parent et al., 1992*b*).

Model Predictions

Simulations were performed to obtain the predictions of the model with respect to: (i) the time course of the presteady-state currents in response to a voltage jump; (ii) the dependence of the charge movement Q—characterized by the Boltzmann parameters z, $V_{0.5}$ and Q_{max}, on membrane voltage and external sodium concentration; and (iii) the dependence of the relaxation time constant τ—characterized by the bell-shaped curve with the parameters τ_{max} and V_{max}, on voltage and external sodium concentration. Figure 7*A* presents the model predictions for the time course of the presteady-state currents as membrane voltage is stepped from −100 to +100 mV. The model predicts that the total presteady-state current (trace *c*) is due to Na^+-binding/dissociation from the transporter (trace *a*) and a conformational change of the empty transporter (trace *b*). Moreover, because Na^+ dissociation from the transporter ($[CNa_2]' \rightleftarrows [C]'$) is much more rapid than the isomerization $[C]' \rightleftarrows [C]''$, there is a transient accumulation of transporters in the $[C]'$ state. Thus the model predicts that the presteady-state currents exhibit a rise to a peak (at 0.5 msec) before relaxing to the steady-state. Figure 7*B* shows the relative contributions of k_{16}, k_{61}, k_{12} and k_{21} to the slow time constant τ. Over the voltage range −50 to +50 mV, at 100 mM $[Na]_o$ the shape of the τ-V curves and both τ_{max} and V_{max} are determined chiefly by conformation changes of the empty transporter — τ_{max} is slightly higher and V_{max} is slightly more positive than expected from k_{16} and k_{61} due to k_{21}. This suggests that to a first approximation the experimental τ_{max} and $V_{\tau max}$ observed in 100 mM $[Na]_o$ are determined by the rate constants k_{16} and k_{61}. At 100 mM $[Na]_o$ the Q-V relation fits a single Boltzmann relation with a $V_{0.5}$ of −10 mV and a z of 1.1 (Fig. 7*C*), and the τ-V curve is bell-shaped with a maximum (τ_{max}) of 19 msec at a voltage $V_{\tau max}$ of +10 mV (Fig. 7*B*). One might expect that the Q-V curve should fit to the sum of two Boltzmann factors owing to the contribution of two processes (Na^+ binding and conformational changes) to charge movements. Simulations, not shown, indicate that the apparent fit to a single Boltzmann is due to the similarity of the $V_{0.5}$s (19 and 11 mV) and zs (1.7 and 1.5) for the two components. At low Na^+ concentrations, for example, at 20 mM $[Na]_o$, there is, as expected, a poor fit to a single Boltzmann factor (Fig. 7*C*). The model also predicts another time constant ($\tau_{fast} << 2$ msec) that is largely beyond the resolution of the 2-electrode voltage clamp (*not shown*), but has been observed in the cut-open oocyte preparation with a time constant of ≈100 μsec and was relatively independent of voltage (Loo, Bezanilla & Wright, 1994).

In the case of the τ-V curves, τ_{max} is predicted to decrease and $V_{\tau max}$ is predicted to become more negative (Fig. 7*B* and *F*). The voltage at the peak of the τ-V curves ($V_{\tau max}$) is close to the midpoint of the Q-V curves ($V_{0.5}$, and the shift in $V_{\tau max}$ (≈30 mV) parallels the shift in $V_{0.5}$ as external Na^+ is reduced from 100 to 20 mM (Fig. 7*B* and *D*). These effects are due to the large decrease in Na^+ binding to the protein (Fig. 7*B*); recall that the rate of Na^+ binding is a quadratic function of $[Na]_o$.

As external Na^+ is reduced from 100 to 10 mM the model predicts that the Q-V curve moves left along the V_m axis, i.e., $V_{0.5}$ moves to more negative potentials, and there is a decrease in the apparent valence of the moveable charge (Fig. 7*C* and *E*). There is also an *apparent* decrease in Q_{max} (Fig. 7*C*) due to: (a) fitting the Q-V curve to a single Boltzmann relation, and (b) the large positive shift in $V_{0.5}$ for Na^+ binding (≈30 mV for a 10-fold change in Na^+). Simulations over a larger volt-

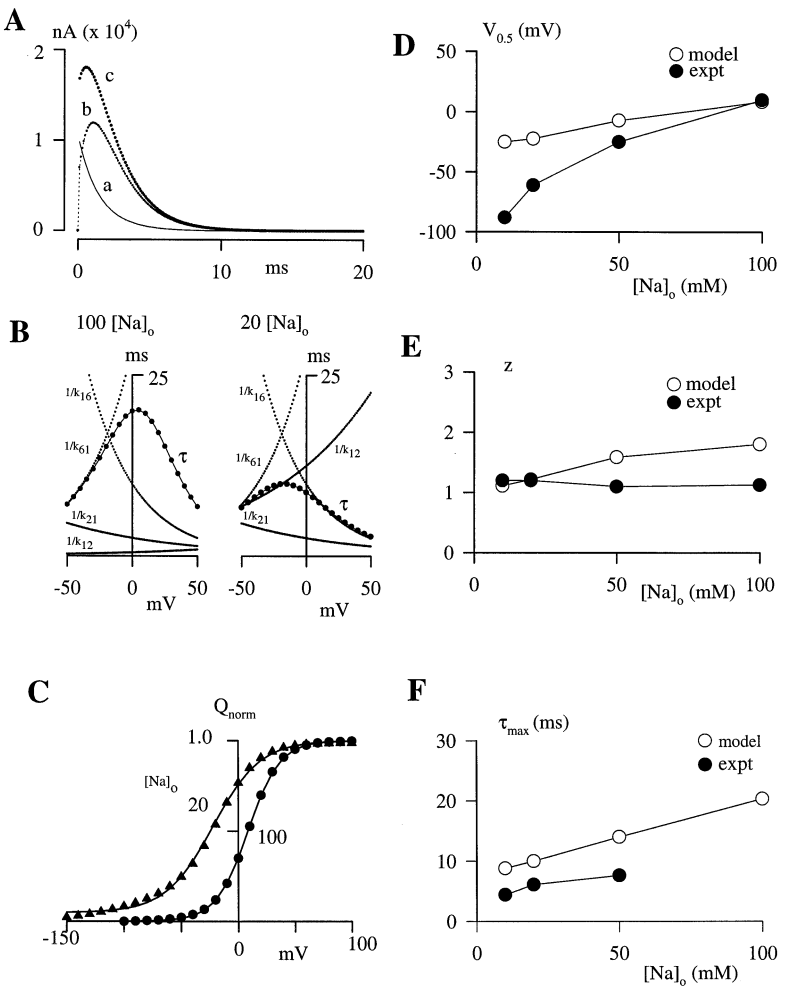

Fig. 7. Model stimulation. Simulation was performed with kinetic parameters from Panayotova-Heiermann et al. (1994). $k_{12}{}^{0}$ = 20,000 sec^{-1} M^{-2}, $k_{21}{}^{o}$ = 400 sec^{-1}, $k_{16}{}^{o}$ = 100 sec^{-1}, $k_{61}{}^{o}$ = 35 sec^{-1}, $\alpha' = 0.3$, $\delta = 0.7$. The total number of transporters was assumed to be 10^{11} and temperature was 20°C. (*A*) The two components and the time course of the presteady-state currents. *a* is the presteady-state current due to Na^+ binding/dissociation from the transporter ($[Na_2]' \rightleftarrows [C]'$); *b* is the current due to the conformational change of the empty transporter ($[C]' \rightleftarrows [C]''$); and *c* is the total presteady-state current obtained by adding *a* and *b*. Notice that *c* rises to a peak before decaying to the steady-state. (*B*) Model simulations of the dependence of the τ-*V* relation on the rate constants k_{12}, k_{21}, k_{16} and k_{61}. The left panel shows the τ-*V* curve at 100 mM $[Na]_o$, and the right panel shows the τ-*V* curve at 20 mM $[Na]_o$. The curves indicated by τ (filled symbols) are model predictions. (*C*) Dependence of the *Q*-*V* relations on $[Na]_o$. At each $[Na]_o$, the *Q*-*V* curves are normalized by Q_{dep} the *Q* at the depolarizing limit, and have been shifted to align at the depolarizing limit. The symbols are predictions of the model and the lines were obtained by fitting the predictions to the Boltzmann relation. (*D*) Dependence of $V_{0.5}$ on $[Na]_o$. (*E*) Dependence of *z* on $[Na]_o$. (*F*) Dependence of τ_{max} on $[Na]_o$. In (*D–F*), the open symbols are the predictions of the model while the filled symbols correspond to experimental values.

age range, experimentally impractical, demonstrate that there is no decrease in Q_{max} as external Na^+ is reduced from 100 to 10 mM (*not shown*).

Predictions *vs.* Experimental Observations

The six-state model for Na^+/glucose cotransport by rSGLT1 and the numerical values estimated by global simulation of the presteady-state and steady-state kinetics (Parent et al., 1992*b;* Panayotova-Heiermann et al., 1994) correctly predict the behavior of rSGLT1 charge movements as functions of time and external $[Na^+]$: (i) The model predicts that the presteady-state currents rapidly rise to a peak before decaying more slowly to the steady state, and this is experimentally observed. The observed time to peak current (3.4 msec, Fig. 1*B*) was longer than the predicted value (0.5 msec, Fig. 7*B*). A large portion of this difference is due to our modeling assumption that the voltage clamp is 'instantaneous' rather than the actual ≈0.8 msec settling time of the amplifier; (ii) As the external $[Na^+]$ is reduced the *Q*-*V* curve moves to more negative potentials (Fig. 7*C*), and, over the voltage range of −150 to +50 mV, there is an apparent reduction in Q_{max}. The observed shift in $V_{0.5}$ (Fig. 7*D*) is less than predicted, the reduction in Q_{max} is larger than predicted, and the apparent valence of the moveable charge (Fig. 7*E*) is less than expected at all but the lowest Na^+ concentrations (10–20 mM).[1] All three deviations are, in part, due to the fitting of the *Q*-*V* data to a single Boltzmann factor over the 10-fold range in external Na^+ concentrations, and the fact that our experimental data are limited by the narrow voltage range that can be studied using the two-electrode voltage clamp in oocytes (−150 to +50 mV). The discrepancy may also be in part due to our simplifying assumption that the binding of 2 Na^+ ions behaves as a single reaction. This may

[1] Previous studies of rabbit SGLT1 indicated that there was no charge movement when the external Na^+ concentration was reduced below 50 mM (Parent et al., 1992*a*). The apparent discrepancy is due to the ''slow'' voltage clamp and the low level of SGLT1 expression in the earlier study.

be correct at high external Na^+ concentrations where one ion binds at a much faster rate that the other, but at low Na^+ concentrations the data suggest that this assumption may not be valid. Heterogeneity of ion binding may be explored in the future by replacing Na^+ with other ions, e.g., H^+, Li^+ and Tb^{3+}, that can substitute for Na^+ in driving Na^+-cotransporters (Hirayama et al., 1995). The valence of 1.2, predicted and observed at the low Na^+ concentrations, is expected for a divalent charge on the protein moving over 60% of the membrane field; and (iii) The effect of external [Na^+] on the shape of the experimental τ-V curves (Fig. 4 and Table 1) is anticipated by our model (Fig. 7*B*). In both cases, the τ-V curves move left along the voltage axis ($V_{\tau max}$ becomes more negative, Fig. 7*B*), and there is a decrease in τ_{max} (Fig. 7*F*). The model also predicted a decrease in τ_{max} with decreasing $[Na]_o$ (Fig. 7*F*) and a shift of $V_{\tau max}$ towards more negative voltages as $[Na]_o$ is decreased (Fig. 7*B*). Examination of the τ-V curves at different Na^+ concentrations and temperatures (Fig. 4) and Table 1 gives strong credence to the predicted behavior.

This extension of our previous studies of human SGLT1 charge movements (Loo et al., 1993), has been possible due to the fact that the charge-voltage relations of rabbit SGLT1 fall more completely within the voltage range of the 2-electrode voltage clamp (+50 to −150 mV). The $V_{0.5}$ for the rabbit Q-V curve at 100 mM NaCl is 50 mV more positive than human. This means that the τ-V curves for rabbit SGLT1 were bell-shaped over the range of Na^+ concentrations and temperatures tested (Fig. 4). This permitted the extraction of two new parameters, τ_{max} and $V_{\tau max}$ (Table 1), and a direct comparison of these with those predicted by the model (Fig. 7*B* and *F*). In terms of our model, the differences between the kinetics of rabbit and human SGLT1 charge movements are simply due to differences in rate constants (rabbit k_{16} 100 sec^{-1}, k_{61} 50 sec^{-1}, k_{12} 20,000 $mole^{-2}sec^{-1}$, k_{21} 400 sec^{-1}; human k_{16} 600, k_{61} 25 sec^{-1}, k_{12} 14,000 $mole^{-2}sec^{-1}$, k_{21} 300 sec^{-1}) caused by difference in the primary sequence of the two isoforms (84% identity, 94% similarity).

Phlorizin

Previously, Birnir et al. (1991) have found that 10 μM phlorizin reduced the sugar-induced steady-state current 50% at all membrane potentials, indicating that phlorizin blockade of the steady-state current was voltage independent. Thus the intrinsic K_i (≈30 μM) for phlorizin blockade of rSGLT1 presteady-state current was greater than the apparent K_i (≈10 μM) for blockade of the sugar-induced steady-state current. Further work is required to understand the action of phlorizin on the cotransporter.

Temperature

Parent and Wright (1993) have studied the temperature dependence of steady-state Na^+/glucose cotransport in the temperature range (20–30°C). They found no changes in the apparent affinity constant $K_{0.5}$ for sugar of Na^+, or the Hill coefficient n. Only changes in the maximal sugar-induced current I_{max} were observed. The temperature coefficient Q_{10} was 2.7–3.3, and corresponds to an Arrhenius (activation) energy of ≈25 kcal/mole. The present results on the temperature dependence of the presteady-state kinetics of SGLT1 show that the maximal charge Q_{max} was independent of temperature, and is expected for charge movement since Q_{max} provides a measure of the number of transporters in the plasma membrane. While z was independent of temperature, the relaxation kinetics of the presteady-state currents was dependent on temperature. Increasing temperature from 20 to 30°C shifted $V_{0.5}$ 25–28 mV towards more negative voltages. Increasing temperature and decreasing Na^+ concentration produced similar effects in decreasing the relaxation time constant τ. If Na^+ binding (i.e., the $K_{0.5}$ for Na^+) is temperature-insensitive as suggested by Parent and Wright (1993), then the shift in $V_{0.5}$ with increasing temperature indicates that k_{16}/k_{61} is temperature dependent, and that temperature had a bigger effect on k_{61} than k_{16}.

Model simulations suggest that there are three main effects of increasing the temperature from 20 to 30°C: (i) the ratio k_{61}/k_{16} was increased 4-fold (from 100 sec^{-1}/35 sec^{-1} to 400 sec^{-1}/35 sec^{-1}) to account for the shift in $V_{0.5}$; (ii) because of the 3-fold increase in maximal sugar-induced current, there was a 3-fold increase in k_{56}, the rate limiting step for steady-state sugar transport at −50 to −150 mV (from 16 sec^{-1} to 50 sec^{-1}); and (iii) the intrinsic dissociation constant for glucose k_{23}/k_{32} was increased about 2-fold (from 100,000 sec^{-1}/20 sec^{-1} to 180,000 sec^{-1}/20 sec^{-1}) while that for Na^+, k_{12}/k_{21} remained unchanged. Interestingly, the Q_{10} for the slow time constant of the presteady-state current (Fig. 4*D*) and the maximal sugar-induced current (Parent & Wright, 1993) were similar (3–4) and correspond to an activation energy of ~25 kcal/mole. Thus there are two steps in the transport cycle which involves conformational changes with high activation energies. Recently, a model has been proposed that cotransporters are single-file ion channels in which multiple-substrates can permeate. The presteady-state currents originate from the movement of the ions in the membrane electric field and conformational changes are not involves (Su et al., 1996). The high activation energies that we have measured would argue against such a mechanism.

Conclusions

We have shown that the rabbit Na^+/glucose cotransporter exhibits presteady-state currents that are sensitive to ex-

ternal Na^+, membrane voltage and temperature, and blocked by phlorizin. The kinetic model predicts that these currents are due to Na^+ binding/dissociation and a conformational change of the empty cotransporter. The model indicates that the slow time constant τ is due to conformational transitions of the empty cotransporter (Fig. 7*B*), thus the kinetics that we have described are due largely to the conformational change of the empty transporter. The model also predicts a much faster time constant τ_{fast} arising from Na^+ binding/dissociation, and which we have observed in preliminary experiments (Loo et al., 1994). Future experiments will involve studying this process at a higher temporal resolution, using the cut-open oocyte preparation (Loo et al., 1994). In addition, since the low affinity Na^+/glucose cotransporter SGLT2 has a stoichiometry of 1 Na^+:1 glucose (Mackenzie et al., 1994, 1995), a comparison of the presteady-state kinetics of SGLT1 and SGLT2 will provide insight into the influence of external Na^+ on the kinetics of presteady-state currents. For example, the model underestimates the magnitude of the shift in $V_{0.5}$ with decreasing Na^+ (Fig. 7*D*), and this may be due to the assumptions on the binding of the 2 Na^+ ions (Parent et al., 1992*b*). Finally, in view of the common general properties of presteady-state currents among cotransporters (Table 2), the kinetic model may be applicable to other cotransporters.

This work was supported by National Institutes of Health Grants DK19567 and NS25554. We thank our colleagues for their helpful comments on the manuscript.

References

Birnir, B., Loo, D.D.F., Wright, E.M. 1991. Voltage-clamp studies of the intestinal Na^+/glucose cotransporter cloned from rabbit small intestine. *Pfluegers Arch.* **418:**79–85

Boorer, K. J., Loo, D.D.F., Wright, E.M. 1994. Kinetics of the H^+/hexose cotransporter (STP1) from *Arabidopsis thaliana* expressed in *Xenopus* oocytes. *J. Biol. Chem.* **269:**20417–20424

Galli, A., DeFelice, L.J., Duke, B.J., Moore, K.R., Blakely, R.D. 1995. Sodium-dependent norepinephrine-induced currents in norepinephrine-transporter-transfected HEK-293 cells blocked by cocaine and antidepressants. *J. Exp. Biol.* **198:**2197–2212

Hager, K., Hazama, A., Kwon, H.M., Loo, D.D.F., Handler, J.S., Wright, E.M. 1995. Kinetics and specificity of the renal Na^+/myo-inositol cotransporter expressed in *Xenopus* oocytes. *J. Membrane Biol.* **143:**103–113

Hediger, M.A., Cody, M.J., Ikeda, T.S., Wright, E.M. 1987. Expression cloning and cDNA sequencing of the Na^+/glucose cotransporter. *Nature* **330:**379–381

Hirayama, B., Loo, D.D.F., Wright, E.M. 1995. Kinetic constraints of cation activation of the Na/glucose cotransporter. *Biophys. J.* **68:**A439

Hirsch, J.R., Loo, D.D.F., Wright, E.M. 1996. Regulation of Na^+/glucose cotransporter expression by protein kinases in *Xenopus* oocytes. *J. Biol. Chem.* **271:**14740–14746

Loo, D.D.F., Bezanilla, F., Wright, E.M. 1994. Two voltage-dependent steps are involved in the partial reactions of the Na^+/glucose cotransporter. *FASEB J.* **8:**A344

Loo, D.D.F., Hazama, A., Supplisson, S., Turk, E., Wright, E.M. 1993. Relaxation kinetics of the Na^+/glucose cotransporter. *Proc. Natl. Acad. Sci USA* **90:**5767–5771

Lostao, M.P., Hirayama, B.A., Loo, D.D.F., Wright, E.M. 1994. Phenylglucosides and the Na^+/glucose cotransporter (SGLT1): Analysis of interactions. *J. Membrane Biol.* **142:**161–170

Mackenzie, B., Loo, D.D.F., Panayotova-Heiermann, M., Wright, E.M. 1995. Kinetics of Na^+/glucose cotransport mediated by SGLT2. *Biophys. J.* **68:**A436

Mackenzie, B., Loo, D.D.F., Fei, Y-J., Liu, W., Ganapathy, V., Leibach, F.H., Wright, E.M. 1996. Mechanisms of the human intestinal H^+-coupled oligopeptide transporter hPEPT1. *J. Biol. Chem.* **271:**5430–5437

Mackenzie, B., Panayotova-Heiermann, M., Loo, D.D.F., Lever, J.E., Wright, E.M. 1994. SAAT1 is a low affinity Na^+/glucose cotransporter and not an amino acid transporter. *J. Biol. Chem.* **269:**22488–22491

Mager, S., Naeve, J., Quick, M., Labarca, C., Davidson, N., Lester, H.A. 1993. Steady states, charge movements, and rates for a cloned GABA transporter expressed in *Xenopus* oocytes. *Neuron* **10:**177–188

Panayotova-Heiermann, M., Loo, D.D.F., Lostao, M.P., Wright, E.M. 1994. Sodium/D-glucose cotransporter charge movements involve polar residues. *J. Biol. Chem.* **269:**21016–21020

Panayotova-Heiermann, M., Loo, D.D.F., Wright, E.M. 1995. Kinetics of steady-state currents and charge movements associated with the rat Na^+/glucose cotransporter. *J. Biol. Chem.* **270:**27099–27105

Parent, L., Supplisson, S., Loo, D.D.F., Wright, E.M. 1992*a*. Electrogenic properties of the cloned Na^+/glucose cotransporter I. voltage-clamp studies. *J. Membrane Biol.* **125:**49–62

Parent, L., Supplisson, S., Loo, D.D.F., Wright, E.M. 1992*b*. Electrogenic properties of the cloned Na^+/glucose cotransporter II. A transport model under nonrapid equilibrium conditions. *J. Membrane Biol.* **125:**63–79

Parent, L., Wright, E.M. 1993. Electrophysiology of the Na^+/glucose cotransporter. In: Molecular Biology and Function of Carrier Proteins. L. Reuss, J.M. Russell, Jr., and M.L. Jennings, editors. pp. 263–281. Rockefeller University Press

Press, W.H., Flannery, B.P., Teukolsky, S.A., Vetterling, W.T. 1986. Numerical Recipes: The Art of Scientific Computing. Cambridge University Press, Cambridge, UK

Su, A., Mager, S., Mayo, S.L., Lester, H.A. 1996. A multi-substrate single-file model for ion-coupled transporters. *Biophys. J.* **70:**762–777

Umbach, J.A., Coady, M.J., Wright, E.M. 1990. Intestinal Na^+/glucose cotransporter expressed in *Xenopus* oocytes is electrogenic. *Biophys. J.* **57:**1217–1224

Wadiche, J.I., Arriza, J.L., Amara, S.G., Kavanaugh, M.P. 1995. Kinetics of a human glutamate transporter. *Neuron* **14:**1019–1027

Zampighi, G.A., Kreman, M., Boorer, K.J., Loo, D.D.F., Bezanilla, F., Chandy, G., Hall, J.E., Wright, E.M. 1995. A method for determining the unitary functional capacity of cloned channels and transporters expressed in *Xenopus* oocytes. *J. Membrane Biol.* **148:**65–78